Vortex beams at high-energy accelerators: generation strategies and measurement techniques

Dmitry Karlovets

ITMO University, St. Petersburg

25.04.2024

d.karlovets@gmail.com

SYSU, Zhuhai


ITMO University,
founded in 1900


Saint Petersburg, founded in 1703

Dostoevsky lived and wrote here

https://en.wikipedia.org/wiki/Crime_and_Punishment_(manga)

Outline

1. Quantum tomography of the evolved states in QFT:
   a. With the plane-wave electrons/protons/ions…
   b. With the generalized measurements
2. Vortex electrons, ions, nuclei,… - generation strategies at accelerators
   a. Magnetized cathode technique
   b. Magnetized stripping foil technique
3. Acceleration of charged particles with vortices and photon emission

The statement
(rather optimistic)

it is possible to obtain twisted photons, electrons, protons, ions, …

in pretty much all QED/QCD/weak processes:

non-linear Thomson/Compton scattering, e-e+ annihilation, Cherenkov emission, etc.

We choose the final states as twisted ones

and calculate the probability

(which can be lower or higher)!

On a deeper level
(moderately optimistic)

1. The choice of the final states implies existence of such a detector

For instance, one can calculate the probability for the generation of gamma-ray vortices via non-linear Compton sc., but how do we make such a detector?

2. Without specifying the detector, one can judge if the state is twisted

via the formalism of evolved states:

$$|e', \gamma\rangle = \left(\hat{1} + \hat{S}^{(1)}\right)|\text{in}\rangle \qquad \hat{S} = \hat{1} + \hat{S}^{(1)} = \hat{1} - ie\int d^4x\, \hat{j}^{\mu}(x)\hat{A}_{\mu}(x)$$

3. Once we know that a twisted state is generated,

we can detect it with whichever detector we have!

The probability to detect a twisted state →

→ the probability <u>amplitude</u> to generate the twisted state

Differences from the standard approach:

1. No dependence on the detector choice: we derive the state as it is
2. The dependence on a phase of an S-matrix element is kept

QFT approach for photon emission

$$e \to e' + \gamma \qquad |e', \gamma\rangle^{(\mathrm{ev})} = \hat{S}^{(1)} |\mathrm{in}\rangle$$

The field operators:

$$\hat{\boldsymbol{A}}(\boldsymbol{r},t) = \sum_{\lambda_\gamma=\pm1} \int \frac{d^3k}{(2\pi)^3} \left(\boldsymbol{A}_{\boldsymbol{k}\lambda_\gamma}(\boldsymbol{r},t)\, \hat{c}_{\boldsymbol{k}\lambda_\gamma} + \mathrm{h.c.} \right),$$

$$\hat{\boldsymbol{E}}(\boldsymbol{r},t) = -\frac{\partial \hat{\boldsymbol{A}}(\boldsymbol{r},t)}{\partial t} = \sum_{\lambda_\gamma=\pm1} \int \frac{d^3k}{(2\pi)^3}\, i\omega \left(\boldsymbol{A}_{\boldsymbol{k}\lambda_\gamma}(\boldsymbol{r},t)\, \hat{c}_{\boldsymbol{k}\lambda_\gamma} - \mathrm{h.c.} \right),$$

$$\hat{\boldsymbol{H}}(\boldsymbol{r},t) = \nabla \times \hat{\boldsymbol{A}}(\boldsymbol{r},t) = \sum_{\lambda_\gamma=\pm1} \int \frac{d^3k}{(2\pi)^3}\, i\mathrm{k} \times \left(\boldsymbol{A}_{\boldsymbol{k}\lambda_\gamma}(\boldsymbol{r},t)\, \hat{c}_{\boldsymbol{k}\lambda_\gamma} - \mathrm{h.c.} \right)$$

$$\boldsymbol{A}_{\boldsymbol{k}\lambda_\gamma}(\boldsymbol{r},t) = \frac{\sqrt{4\pi}}{\sqrt{2\omega}}\, \boldsymbol{e}_{\boldsymbol{k}\lambda_\gamma}\, e^{-i\omega t + i\boldsymbol{k}\cdot\boldsymbol{r}},$$

QFT approach for photon emission

1. The probability amplitude in momentum space:

$$S_{fi}^{(1)} = \langle f_e, f_\gamma | \hat{S}^{(1)} | \text{in} \rangle = \langle \mathbf{p}, \lambda; \mathbf{k}, \lambda_\gamma | \hat{S}^{(1)} | \text{in} \rangle$$

2. The probability amplitude in space-time:

$$\langle 0 | \hat{\psi}(\boldsymbol{r}_e, t_e) \hat{\mathbf{A}}(\boldsymbol{r}_\gamma, t_\gamma) | e', \gamma \rangle^{(\text{ev})}$$

$$|e', \gamma\rangle = \left(\hat{1} + \hat{S}^{(1)}\right) |\text{in}\rangle$$

$$= \int \frac{d^3 p}{(2\pi)^3} \frac{d^3 k}{(2\pi)^3} \sum_{\lambda_\gamma = \pm 1} \sum_{\lambda = \pm 1/2} \frac{\sqrt{4\pi}}{\sqrt{2\omega}} \frac{1}{\sqrt{2\varepsilon}} u_{p\lambda} \boldsymbol{e}_{k\lambda_\gamma} S_{fi}^{(1)} e^{-i\varepsilon t_e + i \boldsymbol{p} \cdot \boldsymbol{r}_e - i\omega t_\gamma + i \boldsymbol{k} \cdot \boldsymbol{r}_\gamma}$$

The 2-particle entangled state:

$$|e', \gamma\rangle = |\mathrm{in}\rangle + \sum_{\lambda'=\pm 1/2, \lambda_\gamma=\pm 1} \int \frac{d^3k}{(2\pi)^3} \frac{d^3p'}{(2\pi)^3} |\mathbf{p}', \lambda'\rangle \otimes |\mathbf{k}, \lambda_\gamma\rangle\, S_{fi}^{(1)}$$

If the electron is detected in a state $\langle f_e^{(\mathrm{det})}|$ the photon evolved state becomes

$$|\gamma\rangle = \langle f_e^{(\mathrm{det})}|e_{\mathrm{in}}\rangle|0_\gamma\rangle + \sum_{\lambda', \lambda_\gamma} \int \frac{d^3k}{(2\pi)^3} \frac{d^3p'}{(2\pi)^3} |\mathbf{k}, \lambda_\gamma\rangle\, (f_e^{(\mathrm{det})}(\mathbf{p}', \lambda'))^*\, S_{fi}^{(1)},$$

The electron detector function

If the electron is a plane wave:

$$\delta(\mathbf{p}'_\perp + \mathbf{k}_\perp) = \delta(p'_x + k_x)\delta(p'_y + k_y) = \frac{1}{p'_\perp}\,\delta(p'_\perp - k_\perp)\left(\delta(\phi' - (\phi_k - \pi))\Big|_{\phi_k \in [\pi, 2\pi]} + \delta(\phi' - (\phi_k + \pi))\Big|_{\phi_k \in [0, \pi]}\right)$$

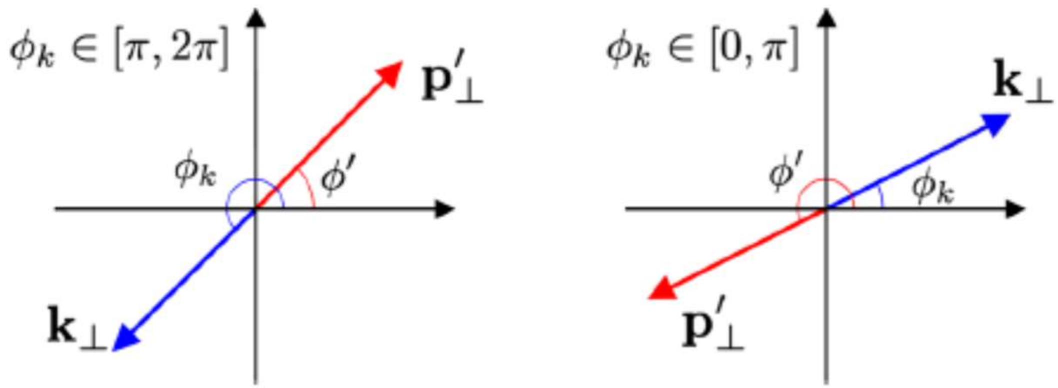

$$|\gamma\rangle = \langle f_e^{(\mathrm{det})}|e_{\mathrm{in}}\rangle|0_\gamma\rangle + \sum_{\lambda',\lambda_\gamma}\int \frac{d^3k}{(2\pi)^3}\frac{d^3p'}{(2\pi)^3}\,|\mathbf{k},\lambda_\gamma\rangle\,(f_e^{(\mathrm{det})}(\mathbf{p}',\lambda'))^*\,S_{fi}^{(1)},$$

3 delta-functions   4 delta-functions

The photon evolved state is a plane wave!

Quantum tomography naturally arises in photon emission

(even if the detected electron is a plane wave)

$$\mathcal{W}(\mathbf{r},t) = \frac{1}{8\pi}\langle\gamma|\hat{\boldsymbol{E}}^2(\boldsymbol{r},t) + \hat{\boldsymbol{H}}^2(\boldsymbol{r},t)|\gamma\rangle - \frac{\varepsilon_0}{4\pi} = \frac{1}{4\pi}\left(\left|\langle 0|\hat{\boldsymbol{E}}(\boldsymbol{r},t)|\gamma\rangle\right|^2 + \left|\langle 0|\hat{\boldsymbol{H}}(\boldsymbol{r},t)|\gamma\rangle\right|^2\right),$$

The vacuum contribution

$$\langle 0|\hat{\boldsymbol{E}}(\boldsymbol{r},t)|\gamma\rangle = \sum_{\lambda_\gamma}\int\frac{d^3k}{(2\pi)^3} i\omega \boldsymbol{A}_{\boldsymbol{k}\lambda_\gamma}(\boldsymbol{r},t)\, S^{(\mathrm{GM})}_{fi}(\mathbf{k},\lambda_\gamma),$$

$$\boldsymbol{A}_{\boldsymbol{k}\lambda_\gamma}(\boldsymbol{r},t) = \frac{\sqrt{4\pi}}{\sqrt{2\omega}}\,\boldsymbol{e}_{\boldsymbol{k}\lambda_\gamma}\, e^{-i\omega t + i\boldsymbol{k}\cdot\boldsymbol{r}},$$

$$S^{(\mathrm{GM})}_{fi}(\mathbf{k},\lambda_\gamma) = \sum_{\lambda'}\int\frac{d^3p'}{(2\pi)^3}\,(f_e^{(\mathrm{det})}(\mathbf{p}',\lambda'))^*\, S^{(1)}_{fi}(\mathbf{p}',\lambda',\mathbf{k},\lambda_\gamma)$$

Quantum tomography naturally arises in photon emission

(even if the detected electron is a plane wave)

$$\frac{1}{4\pi}\left|\langle 0|\hat{\boldsymbol{E}}(\boldsymbol{r},t)|\gamma\rangle\right|^2 = \frac{1}{4\pi}\sum_{\lambda_\gamma,\tilde{\lambda}_\gamma}\int\frac{d^3K}{(2\pi)^3}\frac{d^3k}{(2\pi)^3}\,\boldsymbol{E}^*_{\tilde{\lambda}_\gamma}(\mathbf{K}-\mathbf{k}/2)\cdot\boldsymbol{E}_{\lambda_\gamma}(\mathbf{K}+\mathbf{k}/2)\,e^{-it(\omega(\mathbf{K}+\mathbf{k}/2)-\omega(\mathbf{K}-\mathbf{k}/2))+i\mathbf{r}\cdot\mathbf{k}} =$$

$$= \int\frac{d^3K}{(2\pi)^3}\,\mathcal{W}(\mathbf{r},\mathbf{K},t),$$

The photon Wigner function:

$$\mathcal{W}(\mathbf{r},\mathbf{K},t) = \frac{1}{4\pi}\sum_{\lambda_\gamma,\tilde{\lambda}_\gamma}\int\frac{d^3k}{(2\pi)^3}\,\boldsymbol{E}^*_{\tilde{\lambda}_\gamma}(\mathbf{K}-\mathbf{k}/2)\cdot\boldsymbol{E}_{\lambda_\gamma}(\mathbf{K}+\mathbf{k}/2)\,e^{-it(\omega(\mathbf{K}+\mathbf{k}/2)-\omega(\mathbf{K}-\mathbf{k}/2))+i\mathbf{r}\cdot\mathbf{k}},$$

$$\boldsymbol{E}_{\lambda_\gamma}(\mathbf{k}) = \frac{i\omega\sqrt{4\pi}}{\sqrt{2\omega n^2}}\,e_{\mathbf{k}\lambda_\gamma}\sum_{\lambda}\int\frac{d^3p}{(2\pi)^3}\,f_e^{(\text{in})}(\mathbf{p},\lambda)S^{(1)}_{fi}(\mathbf{p},\lambda,\mathbf{k},\lambda_\gamma)$$

The first marginal distribution:

$$\int d^3x\, \mathcal{W}(\mathbf{r},\mathbf{K},t) = \frac{\omega}{2n^2}\left|\sum_\lambda \int \frac{d^3p}{(2\pi)^3} f_e^{(\mathrm{in})}(\mathbf{p},\lambda) S_{fi}^{(1)}(\mathbf{p},\lambda,\mathbf{k},\lambda_\gamma)\right|^2 =$$

$$= \frac{\omega}{2n^2}(2\pi)^2\frac{T}{2\pi}\delta(\varepsilon(\mathbf{p})-\varepsilon'-\omega)\,\frac{4\pi}{2\omega(\mathbf{k})n^2(\omega(\mathbf{k}))2\varepsilon(\mathbf{p})2\varepsilon'(\mathbf{p}')}\left|\sum_\lambda f_e^{(\mathrm{in})}(\mathbf{p},\lambda)\, M_{fi}(\mathbf{p},\mathbf{k},\lambda,\lambda_\gamma)\right|^2_{\mathbf{p}=\mathbf{p}'+\mathbf{k}}$$

The customary probability in momentum space!

The second marginal distribution:

$$\int \frac{d^3K}{(2\pi)^3}\mathcal{W}(\mathbf{r},\mathbf{K},t) = \frac{1}{4\pi}\left|\langle 0|\hat{\boldsymbol{E}}(\boldsymbol{r},t)|\gamma\rangle\right|^2$$

The probability in space-time!

Quantum tomography naturally arises in photon emission

(even if the detected electron is a plane wave)

1. The energy density of the photon evolved state in space-time depends on the shape of the incoming electron packet:

a snapshot of the electron wave function!

$$\frac{1}{4\pi}\left|\langle 0|\hat{\boldsymbol{E}}(\boldsymbol{r},t)|\gamma\rangle\right|^2 \propto \left|\psi_e^{(\mathrm{in})}(\boldsymbol{r},t)\right|^2$$

2. Complementary measurements – the phase space and the Wigner functions come into play!

Now let's detect the electron in the generalized measurement scheme

1. Projective (von Neumann) measurements: the errors are vanishing
2. Generalized (realistic) measurements: some errors can be finite:
   a. Without the loss of information
   b. With the loss of information

The electron is detected in a state

$$|e'\rangle = \int \frac{d^3 p'}{(2\pi)^3} f_p(\mathbf{p}')|\mathbf{p}', \lambda'\rangle$$

The detector function can be of the Gaussian form:

$$f_p(\mathbf{p}') \propto \prod_i \exp\left\{-(p'_i - \langle p_i\rangle)^2/(2\sigma_i)^2\right\}$$

Generation of vortex particles via generalized measurements

Consider 2 → 2 scattering/annihilation:
en → en, np → np, ep → ep, e+mu → e+mu, etc.

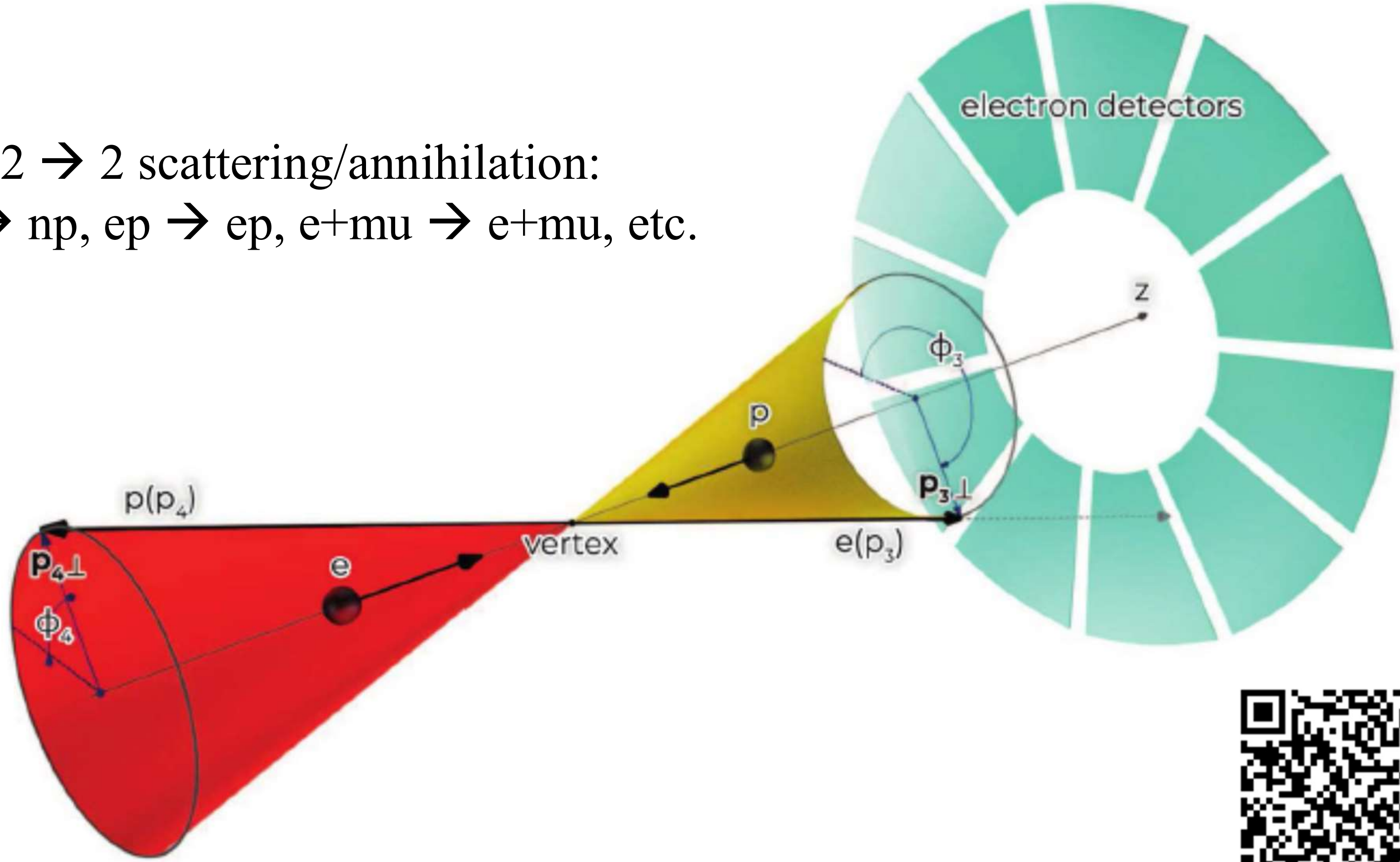

Generation of vortex particles via generalized measurements

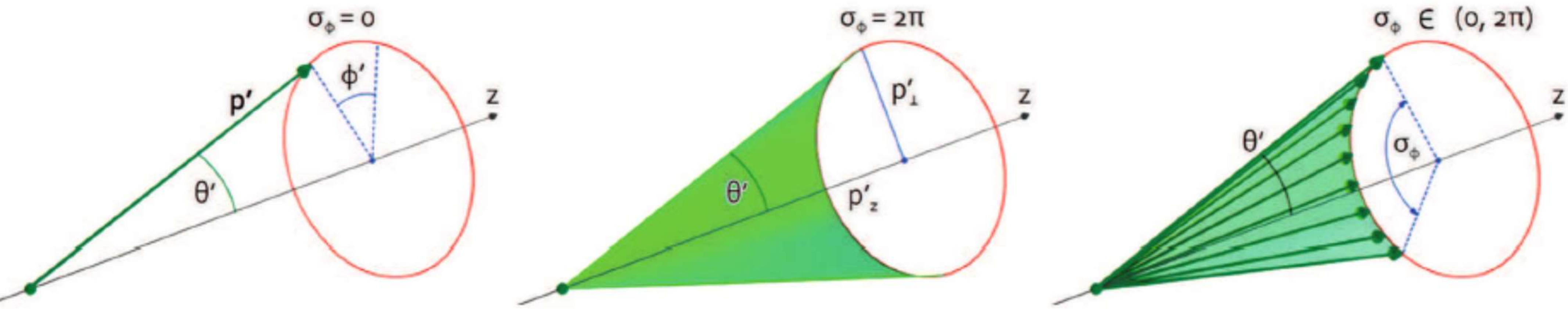

Projective: a plane-wave state

Projective: a Bessel beam

Generalized: a Bessel-like wave packet

D.K., et al., Eur. Phys. J. C 83, 372 (2023)

Generation of vortex particles via generalized measurements

When the uncertainty approaches 2 pi:

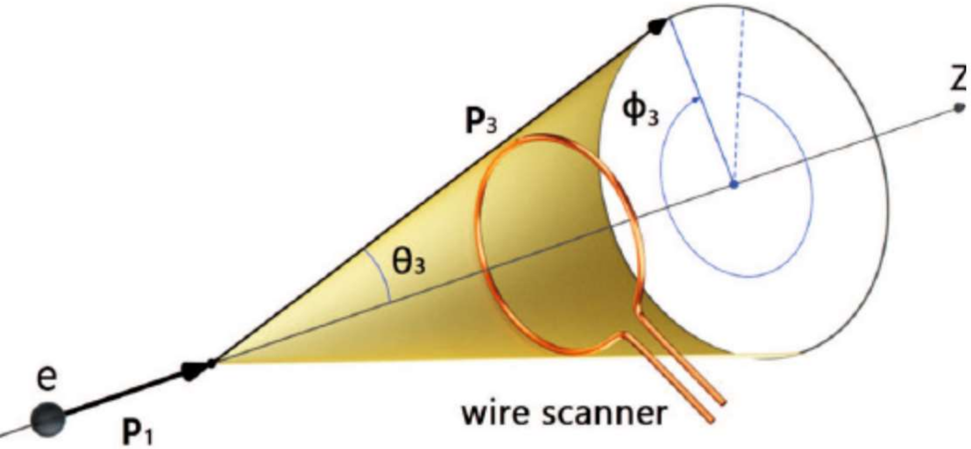

Cherenkov radiation:
the electron scattering angle
is ~ 10^-6 – 10^-5 rad!

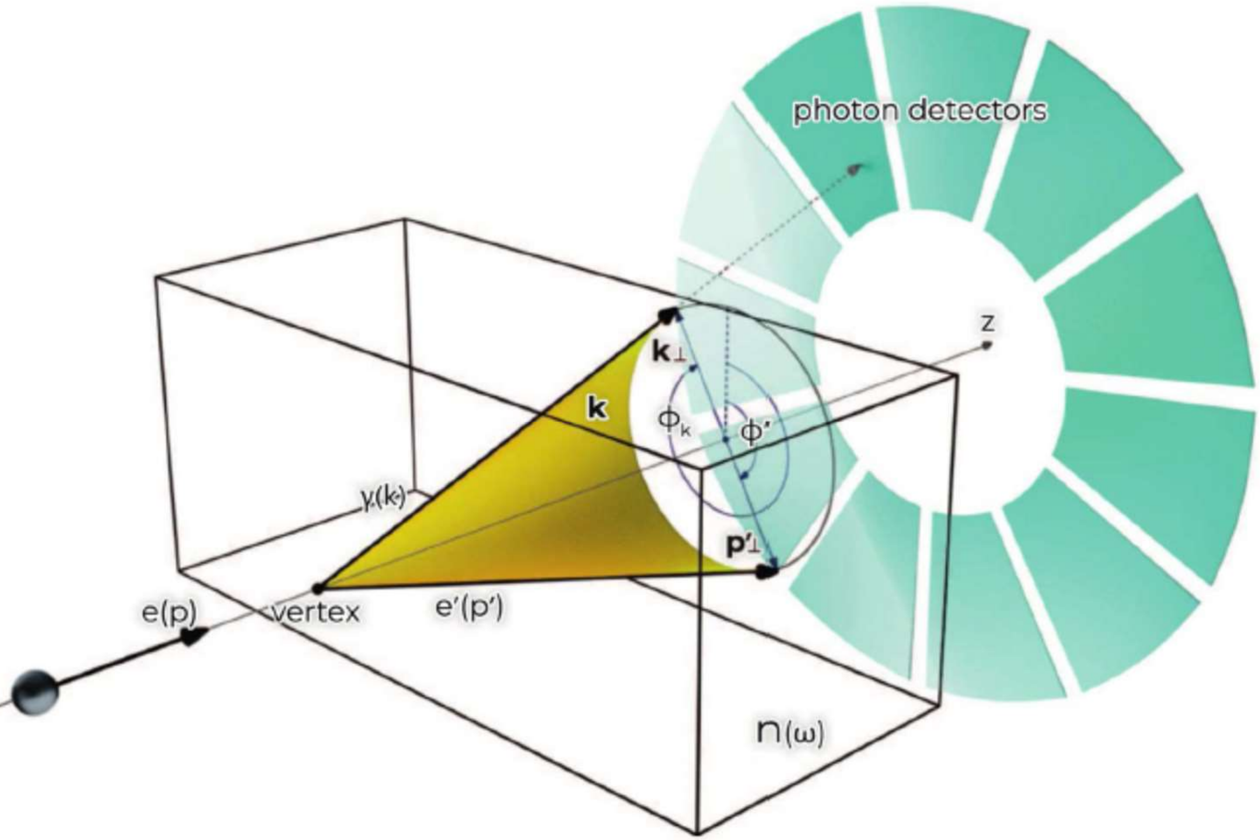

D.K., et al., Eur. Phys. J. C 83, 372 (2023)

First Observation of Photons Carrying Orbital Angular Momentum in Undulator Radiation

J. Bahrdt, K. Holldack, P. Kuske, R. Müller, M. Scheer, and P. Schmid
Helmholtz-Zentrum Berlin, Albert-Einstein-Straße 15, 12489 Berlin, Germany
(Received 26 February 2013; published 15 July 2013)

Photon beams of 99 eV energy carrying orbital angular momentum (OAM) have been observed in the 2nd harmonic off-axis radiation of a helical undulator at the 3rd generation synchrotron radiation light source BESSY II. For detection, the OAM carrying photon beam was superimposed with a reference beam without OAM. The interference pattern, a spiral intensity distribution, was recorded in a plane perpendicular to the propagation direction. The orientation of the observed spiral structure is related to the helicity of the undulator radiation. Excellent agreement between measurements and simulations has been found.

DOI: 10.1103/PhysRevLett.111.034801

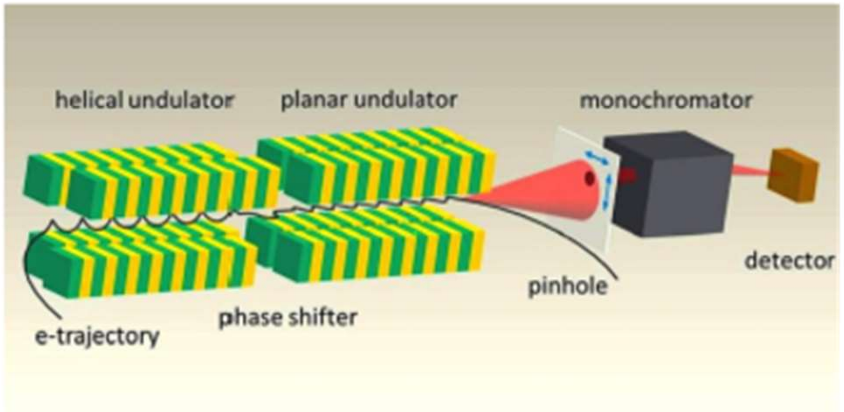

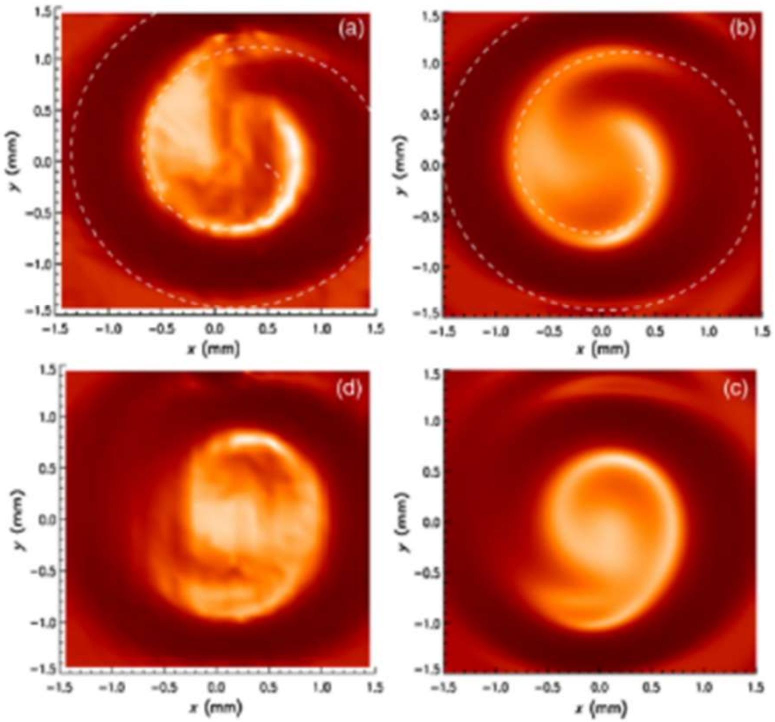

Here we have an effective projection to the state with the OAM=0,

detected at the vanishing scattering angle

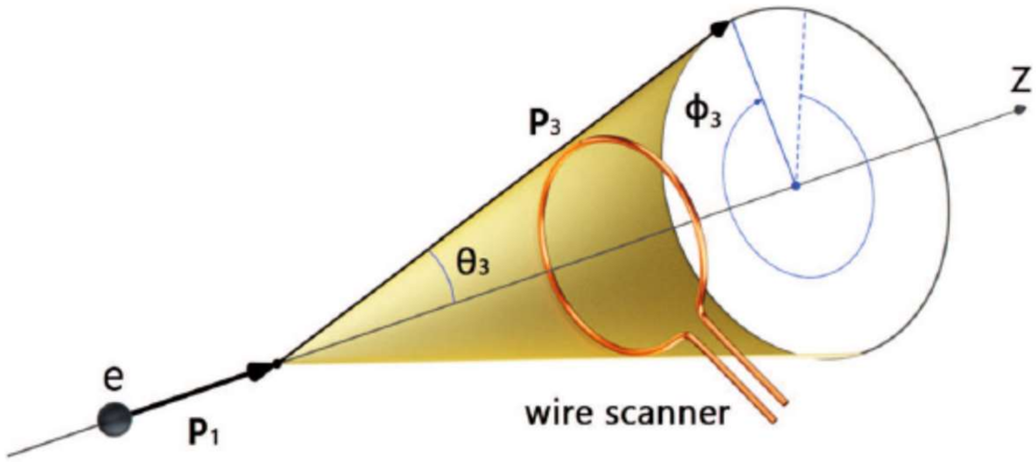

Undulator radiation at XFEL:

the electron scattering angles are ~ 10^-6 – 10^-3 rad!

Generation of vortex particles via generalized measurements

When the uncertainty approaches 2 pi:

$$\mathbf{A}^{(\mathrm{ev})}(\mathbf{k}, \omega) = \int\limits_0^{2\pi} \frac{d\phi'}{2\pi} \sum_{\lambda_\gamma = \pm 1} e\, S_{fi}^{(\mathrm{pw})}$$

The vector potential of the evolved state

Example 1: Cherenkov radiation

$$\hat{j}_z^{(\gamma)} \mathbf{A}^{(\mathrm{ev})} = (\lambda - \lambda') \mathbf{A}^{(\mathrm{ev})},$$

Example 2: Non-linear Compton scattering at the s-th harmonic/helical undulator

$$\hat{j}_z^{(\gamma)} \mathbf{A}_{(\mathrm{g})}^{(\mathrm{ev},s)} = (s + \lambda - \lambda') \mathbf{A}_{(\mathrm{g})}^{(\mathrm{ev},s)},$$ - with a Volkov electron

$$\hat{j}_z^{(\gamma)} \mathbf{A}_{(\mathrm{g})}^{(f,s)} = (s + m - \lambda') \mathbf{A}_{(\mathrm{g})}^{(f,s)},$$ - with a Bessel-Volkov electron

D.K., et al., Eur. Phys. J. C 83, 372 (2023)

A POVM scheme: does the loss of information destroy the photon vorticity?

$$\hat{\rho}_\gamma^{(\mathrm{POVM})} = \mathrm{Tr}\{\hat{F}_e^{(\mathrm{det})}\,\hat{\rho}_{e\gamma}\}$$

If the plane-wave detector is used:

$$\hat{F}_e^{(\mathrm{det})} = \sum_{\lambda'}\int \frac{d^3p'}{(2\pi)^3}\,F_e^{(\mathrm{det})}(\mathbf{p}',\lambda')\,|\mathbf{p}',\lambda'\rangle\langle\mathbf{p}',\lambda'|,$$

$$\hat{\rho}_\gamma = T\sum_{\lambda',\lambda_\gamma,\lambda'_\gamma}\int d\Gamma\,F_e^{(\mathrm{det})}(\mathbf{p}',\lambda')\,T_{fi}^{(\lambda'\lambda_\gamma)}\left(T_{fi}^{(\lambda'\lambda'_\gamma)}\right)^*|\mathbf{k},\lambda_\gamma\rangle\langle\mathbf{k},\lambda'_\gamma|, \Rightarrow \langle\hat{J}_z\rangle = 0$$

For a cylindrical-basis detector:

$$\hat{F}_{tw-e}^{(\mathrm{det})} = \sum_{m'=-\infty}^{\infty}\sum_{\lambda'}\int\frac{dp'_z}{2\pi}\frac{p'_\perp\,dp'_\perp}{2\pi}\,F_{tw-e}^{(\mathrm{det})}(p'_z,p'_\perp,m',\lambda')\,|p'_z,p'_\perp,m',\lambda'\rangle\langle p'_z,p'_\perp,m',\lambda'| \Rightarrow \langle\hat{J}_z\rangle \neq 0$$

Even with the loss of information,
the twisted photons are still generated!

Vortex electrons, ions, nuclei,… - generation strategies at accelerators

Planar-to-circular beam adapters:
analogous to Hermite-Gaussian → Laguerre-Gaussian conversion of light

- Round beams for circular colliders:

elimination of betatron resonances, increase of the beam lifetime.

- Flat beams for linear colliders:

to increase the luminosity and to suppress the beamstrahlung, and to enhance the efficiency of generation of em radiation from X-rays to THz (say, for Smith-Purcell radiation).

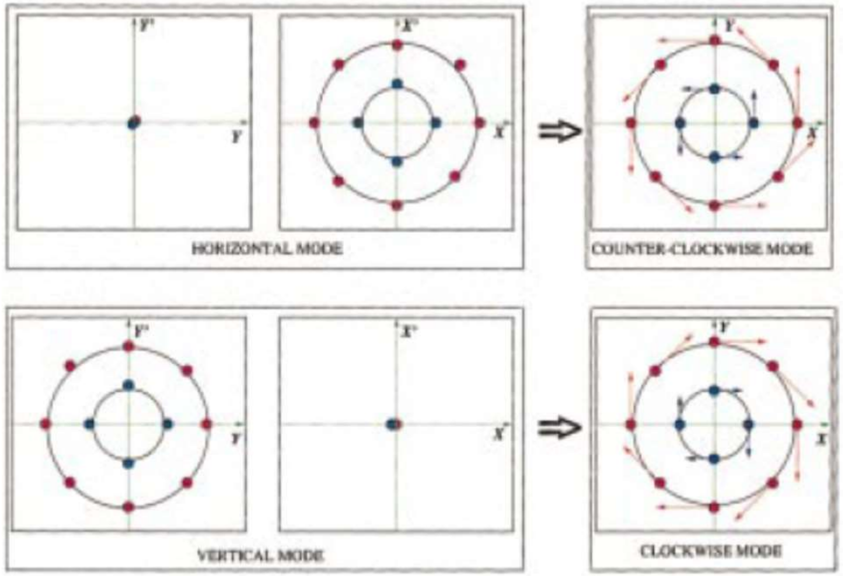

Burov A, Nagaitsev S and Derbenev Y, *Phys. Rev.* E **66** 016503, 2002

6. *Berechnung der Bahn von Kathodenstrahlen im axialsymmetrischen elektromagnetischen Felde;* von H. Busch

Vor einiger Zeit habe ich eine Methode der e/m-Bestimmung angegeben[1]), die — ursprünglich nur zu Unterrichtszwecken ausgearbeitet — sich im Laufe der Versuche als sehr geeignet zu Präzisionsmessungen erwies.[2]) Im folgenden sollen die theoretischen Grundlagen der Methode mitgeteilt werden.

Das Meßverfahren beruht auf der bekannten Erscheinung, daß ein von einem Punkte P ausgehendes divergentes Kathodenstrahlbündel durch ein longitudinales, d. h. parallel zur Bündelachse gerichtetes Magnetfeld wieder in einem Punkte P' vereinigt, „fokussiert" wird. Aus der Entfernung l zwischen Brennpunkt P' und Ausgangspunkt P in Verbindung mit der Stärke $\mathfrak{H}$ des Magnetfeldes erhält man eine Beziehung zwischen der Elektronengeschwindigkeit v und ihrer spezifischen Ladung $\eta = \frac{e}{m}$, die, in üblicher Weise mit einer zweiten, etwa aus dem von den Elektronen durchfallenen Entladungspotential V zu gewinnenden Gleichung kombiniert, η und v einzeln zu berechnen gestattet.

Im Falle eines homogenen Magnetfeldes ist jene Beziehung sehr einfach; hier bilden die Elektronenbahnen die bekannten regelmäßigen Schraubenlinien und die besagte Beziehung lautet:

$$l = \frac{2\pi v}{\eta \mathfrak{H}} \cos\alpha, \tag{1}$$

worin α den Winkel bedeutet, den die Anfangsrichtung der Elektronenbahn mit $\mathfrak{H}$ bildet.[3])

1) H. Busch, Physik. Ztschr. 23. S. 438. 1922.

2) Eine solche Präzisionsbestimmung ist im hiesigen Physikalischen Institut im Gange und steht kurz vor dem Abschluß.

3) Zu beachten ist, daß wegen des Faktors $\cos\alpha$ die Abbildung des Punktes P in P' — in der Sprache der geometrischen Optik — nicht

Busch H 1926 Berechnung der Bahn von Kathodenstrahlen im axialsymmetrischen elektromagnetischen Felde *Ann. Phys.* **386** 974

The Busch theorem: a charged beam/particle in magnetic field gets vorticity

$$\hat{H} = \frac{(\hat{\boldsymbol{p}}^{\mathrm{kin}})^2}{2m} = \frac{(\hat{\boldsymbol{p}}^{\mathrm{can}})^2}{2m} - \omega_{\mathrm{L}} \hat{L}_z^{\mathrm{can}} + \frac{m}{2}\omega_{\mathrm{L}}^2 \rho^2$$

$$\hat{\boldsymbol{p}}^{\mathrm{can}} = \hat{\boldsymbol{p}}^{\mathrm{kin}} + e\boldsymbol{A} = -\mathrm{i}\nabla$$

$$\hat{\boldsymbol{L}}^{\mathrm{can}} = \boldsymbol{r} \times \hat{\boldsymbol{p}}^{\mathrm{can}} \quad \text{and} \quad \hat{\boldsymbol{L}}^{\mathrm{kin}} = \boldsymbol{r} \times \hat{\boldsymbol{p}}^{\mathrm{kin}}$$

$$\langle \hat{L}_z^{\mathrm{kin}} \rangle = \ell - m\omega_{\mathrm{L}} \langle \rho^2 \rangle = \ell - 2\,\mathrm{sgn}(e) \frac{\langle \rho^2 \rangle}{\rho_{\mathrm{H}}^2} \qquad \rho_{\mathrm{H}} = \sqrt{\frac{4}{|e|H}} = 2\lambda_{\mathrm{c}} \sqrt{\frac{H_{\mathrm{c}}}{H}}$$

In quantum mechanics, the canonic OAM is an integer:

$$\langle \hat{L}_z^{\mathrm{can}} \rangle = \ell, \quad \ell = 0, \pm 1, \pm 2, \ldots \qquad (\hbar = 1)$$

The Busch theorem:
a charged beam/particle in magnetic field gets vorticity

$$\langle \hat{L}_z^{\rm kin} \rangle = 0 \quad \Rightarrow \quad \ell = \frac{eH}{2}\langle \rho^2 \rangle = 2\,\mathrm{sgn}(e)\,\frac{\langle \rho^2 \rangle}{\rho_{\rm H}^2} = \frac{1}{2}\,\mathrm{sgn}(e)\,\frac{\langle \rho^2 \rangle}{\lambda_{\rm c}^2}\,\frac{H}{H_{\rm c}},$$

The flux of the field through the area of the beam (classical) or of the wave packet (quantum):

$$\langle \Phi \rangle = H\pi \langle \rho^2 \rangle$$

Akin to the Aharonov-Bohm effect:

$$\Psi \to \Psi\,\exp\left\{ i\theta \frac{q}{2\pi\hbar}\left\langle \oint A dl \right\rangle \right\} = \Psi\, e^{i\ell\theta}$$

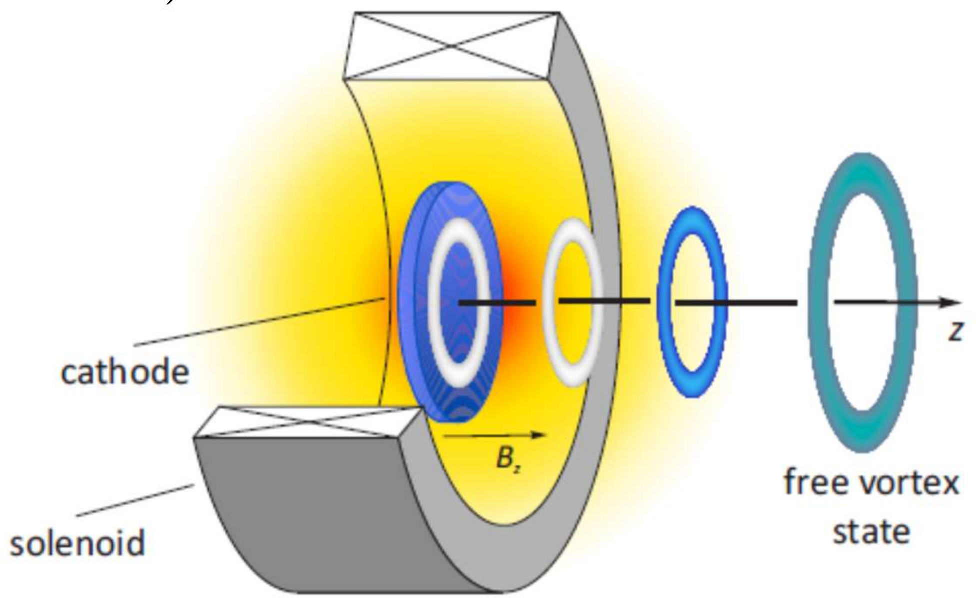

PHYSICAL REVIEW SPECIAL TOPICS - ACCELERATORS AND BEAMS **7**, 123501 (2004)

Generation of angular-momentum-dominated electron beams from a photoinjector

Y.-E Sun,[1,*] P. Piot,[2,†] K.-J. Kim,[1,3] N. Barov,[4,‡] S. Lidia,[5] J. Santucci,[2] R. Tikhoplav,[6] and J. Wennerberg[2,§]
[1]*University of Chicago, Chicago, Illinois 60637, USA*
[2]*Fermi National Accelerator Laboratory, Batavia, Illinois 60510, USA*
[3]*Argonne National Laboratory, Argonne, Illinois 60439, USA*
[4]*Northern Illinois University, DeKalb, Illinois 60115, USA*
[5]*Lawrence Berkeley National Laboratory, Berkeley, California 94720, USA*
[6]*University of Rochester, Rochester, New York 14627, USA*
(Received 2 November 2004; published 22 December 2004)

Various projects under study require an angular-momentum-dominated electron beam generated by a photoinjector. Some of the proposals directly use the angular-momentum-dominated beams (e.g., electron cooling of heavy ions), while others require the beam to be transformed into a flat beam (e.g., possible electron injectors for light sources and linear colliders). In th
an angular-momentum-dominated beam produced in a ph
angular momentum on initial conditions. We also briefly dis
results of the experiment, carried out at the Fermilab/NICAI
in good agreement with theoretical and numerical models.

DOI: 10.1103/PhysRevSTAB.7.123501

Up to <L> ~ 10^8*ħ!

- UV laser, cesium telluride photocathode
- e: **4 MeV/c → 16 MeV/c** after the booster cavity

<L> is conserved during the acceleration!

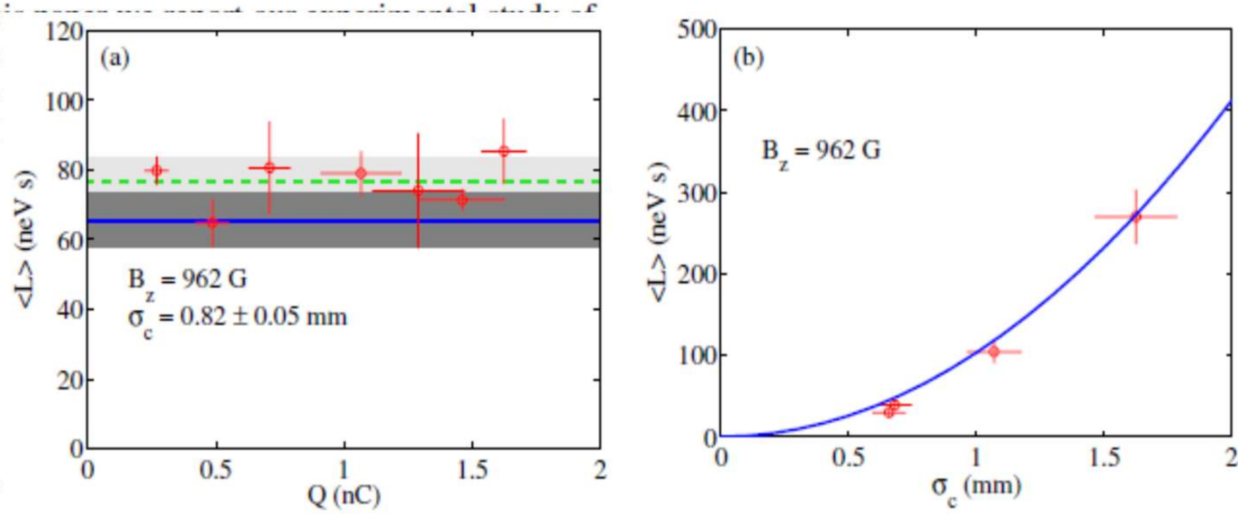

Canonical angular momentum versus charge (a) and photocathode drive-laser beam spot size (b)

Electron wave packets: reference numbers

The rms-radii in SEMs, TEMs, electron accelerators, photo-electrons, etc.:

$$\sqrt{\langle\rho^2\rangle} \sim \textbf{1-100 nm}$$

Example 1: a radius of the ground Landau state in the field H ~ 0.1-10 T is

$$\rho_{\mathrm{H}} = \sqrt{\frac{4}{|e|H}} \sim \textbf{10-100 nm}$$

Example 2: the transverse coherence length of an electron
from a Tungsten photo-cathode or a field-emitter (at room temperature) is*

$$\sqrt{\langle\rho^2\rangle} \sim \textbf{0.5 - 1 nm}$$

*Ehberger D, et al., Phys. Rev. Lett. **114,** 227601 (2015)

PRL 114, 227601 (2015) PHYSICAL REVIEW LETTERS week ending 5 JUNE 2015

Highly Coherent Electron Beam from a Laser-Triggered Tungsten Needle Tip

Dominik Ehberger,[1,2,*] Jakob Hammer,[1,2] Max Eisele,[2,†] Michael Krüger,[1,2,‡] Jonathan Noe,[3] Alexander Högele,[3] and Peter Hommelhoff[1,2,4,§]

[1]Department of Physics, Friedrich Alexander University Erlangen-Nuremberg, Staudtstrasse 1, D-91058 Erlangen, Germany, EU

[2]Max Planck Institute of Quantum Optics, Hans-Kopfermann-Strasse 1, D-85748 Garching/Munich, Germany, EU

[3]Fakultät für Physik and Center for NanoScience (CeNS), Ludwig-Maximilians-Universität München, Geschwister-Scholl-Platz 1, 80539 München, Germany, EU

[4]Max Planck Institute for the Science of Light, Günther-Scharowsky-Strasse 1/ Building 24, D-91058 Erlangen, Germany, EU

(Received 10 December 2014; published 5 June 2015)

We report on a quantitative measurement of the spatial coherence of electrons emitted from a sharp metal needle tip. We investigate the coherence in photoemission triggered by a near-ultraviolet laser with a photon energy of 3.1 eV and compare it to dc-field emission. A carbon nanotube is brought into close proximity to the emitter tip to act as an electrostatic biprism. From the resulting electron matter wave interference fringes, we deduce an upper limit of the effective source radius both in laser-triggered and dc-field emission mode, which quantifies the spatial coherence of the emitted electron beam. We obtain (0.80 ± 0.05) nm in laser-triggered and (0.55 ± 0.02) nm in dc-field emission mode, revealing that the outstanding coherence properties of electron beams from needle tip field emitters are largely maintained in laser-induced emission. In addition, the relative coherence width of 0.36 of the photoemitted electron beam is the largest observed so far. The preservation of electronic coherence during emission as well as ramifications for time-resolved electron imaging techniques are discussed.

van Cittert–Zernicke theorem

$$r_{\text{eff}} = \frac{\lambda_{\text{dB}} \cdot l_{s\text{-}d}}{\pi \cdot \xi_{\perp}}$$

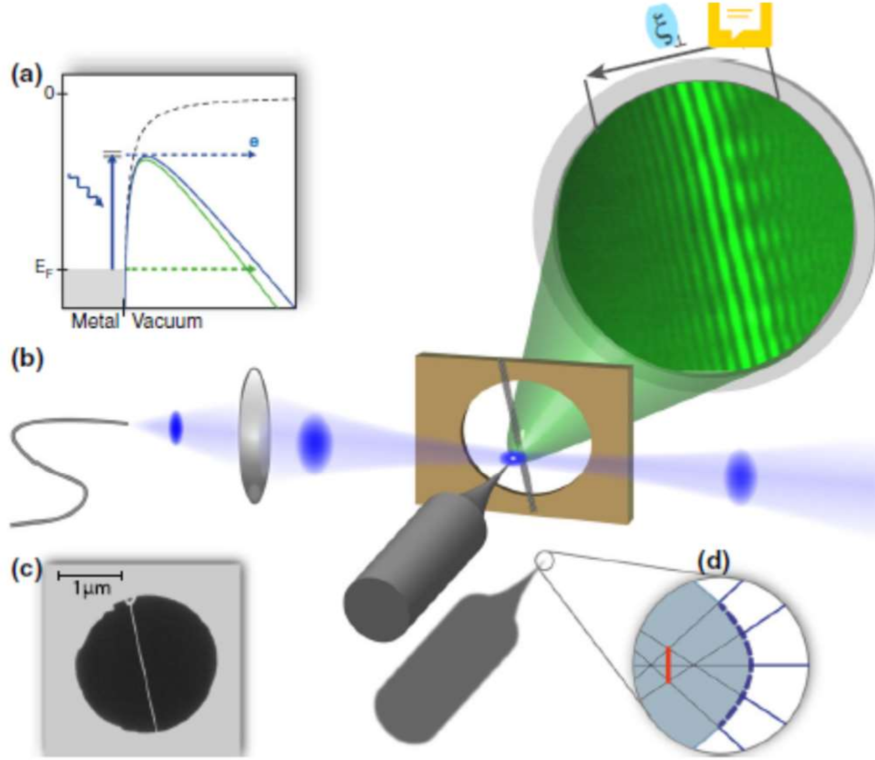

“We use a freestanding carbon nanotube (CNT) as an electron beam splitter, which acts as a biprism filament with nanometer radius”

At room temperature!

The Busch theorem: a charged beam/particle in magnetic field gets vorticity

The realistic estimate:

$$|q| = |eZ| \qquad |\ell| \approx 1.5 \times 10^{-3}\,|Z|\langle r^2\rangle[\mathrm{nm}^2]\,|B_{z,0}|[\mathrm{T}],$$

For electrons

- H > 100 T for Tungsten at room temperature,
- Or to cool the emitter down to ~10 K: the electron inelastic mean free path in metals is ~ 10 nm - 1000 nm for of 3.5–178 K,
- Or to employ special cathodes: GaAs, ring-shaped, photo-cathode with a twisted laser, etc.

Floettmann, DK., PRA **102**, 043517 (2020); DK., New J. Phys. **23** (2021) 033048

The Busch theorem:
a charged beam/particle in magnetic field gets vorticity

1. The photon OAM can be transferred to photo-electrons

The talk by Alisa Chaikovskaia on Saturday!

2. The electron transverse coherence length can correlate with that of the photon
3. The pulsed magnetic field higher than 1 T can be used; it is required only in the generation region!

4. Photocathodes with a ring-shaped emissive area on a non-emissive background (also, for field emission!) can be used

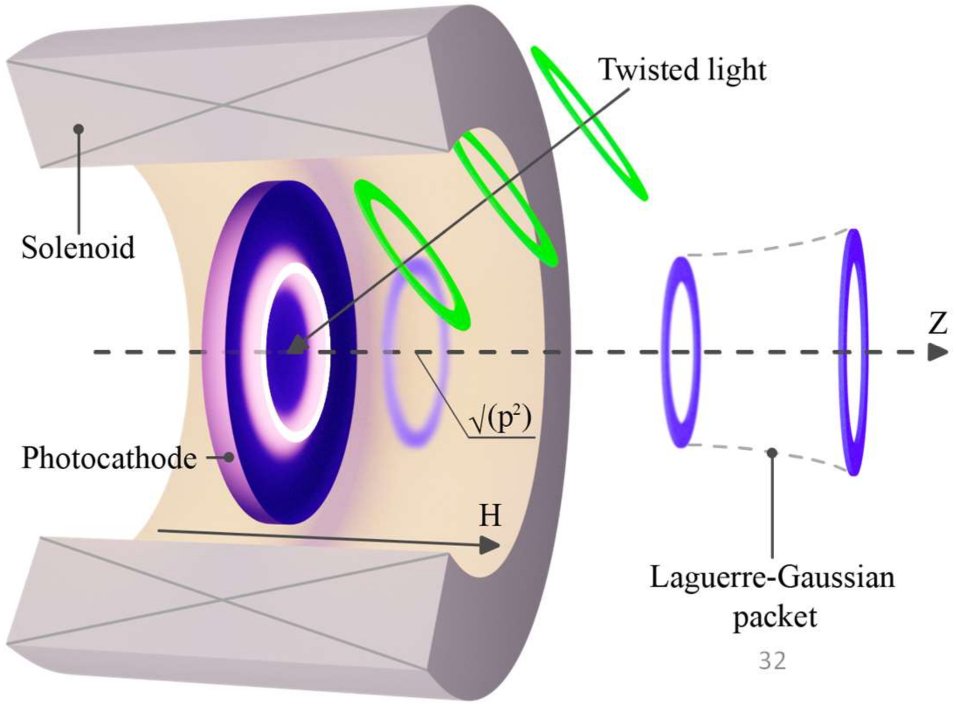

Magnetized stripping foil technique for ions

PRL **113**, 264802 (2014) PHYSICAL REVIEW LETTERS week ending 31 DECEMBER 2014

Experimental Proof of Adjustable Single-Knob Ion Beam Emittance Partitioning

L. Groening,* M. Maier, C. Xiao, L. Dahl, P. Gerhard, O. K. Kester, S. Mickat, H. Vormann, and M. Vossberg
GSI Helmholtzzentrum für Schwerionenforschung GmbH, Darmstadt D-64291, Germany

M. Chung
Ulsan National Institute of Science and Technology, Ulsan 698-798, Republic of Korea
(Received 26 September 2014; published 30 December 2014)

The performance of accelerators profits from phase-space tailoring by coupling of degrees of fre
Previously applied techniques swap the emittances among the three degrees but the set of ava
emittances is fixed. In contrast to these emittance exchange scenarios, the emittance transfer sc
presented here allows for arbitrarily changing the set of emittances as long as the product of the emit
is preserved. This Letter is the first experimental demonstration of transverse emittance transfer
an ion beam line. The amount of transfer is chosen by setting just one single magnetic field
The envelope functions (beta) and slopes (alpha) of the finally uncorrelated and repartitioned be
the exit of the transfer line do not depend on the amount of transfer.

Nitrogen: Z from +3 to +7

The foil (carbon, 200 $\mu g/cm^2$, 30 mm in diameter)

The energies: from 10s to 100s MeV/u

Nuclear Instruments and Methods in Physics Research A 767 (2014) 153–158

Contents lists available at ScienceDirect

Nuclear Instruments and Methods in Physics Research A

journal homepage: www.elsevier.com/locate/nima

ELSEVIER

Minimization of the emittance growth of multi-charge particle beams in the charge stripping section of RAON

CrossMark

Ji-Gwang Hwang [a], Eun-San Kim [a,*], Hye-Jin Kim [b,*], Dong-O Jeon [b]

[a] *Department of Physics, Kyungpook National University, Daegu 702-701, Korea*
[b] *Rare Isotope Science Project, Institute for Basic Science, Jeonmin-dong, Yuseong-gu, Daejeon, Korea*

ARTICLE INFO

Article history:
Received 20 April 2014
Received in revised form
26 July 2014
Accepted 13 August 2014
Available online 21 August 2014

Keywords:
Rare Isotope Science Project
Beam dynamics for multicharge particles
Emittance growth in dispersive section
Correction of high-order aberration

ABSTRACT

The charge stripping section of the Rare isotope Accelerator Of Newness (RAON), which is one of the critical components to achieve a high power of 400 kW with a short lianc, is a source of transverse emittance growth. The dominant effects are the angular straggling in the charge stripper required to increase the charge state of the beam and chromatic aberrations in the dispersive section required to separate the selected ion beam from the various ion beams produced in the stripper. Since the main source of transverse emittance growth in the stripper is the angular straggling, it can be compensated for by changing the angle of the phase ellipse. Therefore the emittance growth is minimized by optimizing the Twiss parameters at the stripper. The emittance growth in the charge selection section is also minimized by the correction of high-order aberrations using six sextupole magnets. In this paper, we present a method to minimize the transverse emittance growth in the stripper by changing the Twiss parameters and in the charge selection section by using sextupole magnets.

Uranium: Z from +33-34 to +77-81

Magnetized stripping foil technique for ions

The quantum Busch theorem for ions:

$$\ell = \frac{q_{\text{out}} - q_{\text{in}}}{2} H \langle \rho^2 \rangle = (Z_{\text{out}} - Z_{\text{in}}) \frac{eH}{2} \langle \rho^2 \rangle$$

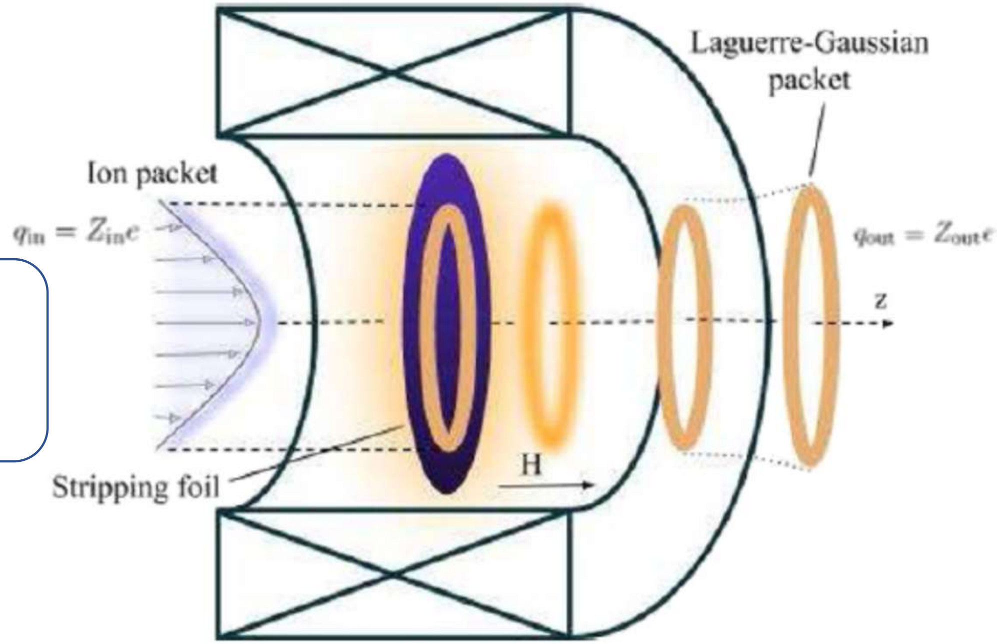

Requirements:

- Negligible space charge (no Coulomb repulsion)
- The transverse coherence larger than 100 nm at H ~ 1 T
- No emittance degradation: small scattering in the target

Magnetized stripping foil technique for ions

The general spreading law is

$$\langle \rho^2 \rangle(t) = \langle \rho^2 \rangle(0) + \frac{\partial \langle \rho^2 \rangle(0)}{\partial t} t + \langle u_\perp^2 \rangle t^2,$$

For the LG packet in the far-field (<z> >> z_R):

$$\boxed{\langle z \rangle = \frac{\langle p \rangle}{2n + |\ell| + 1} \sqrt{\langle \rho^2 \rangle(\langle z \rangle)} \sqrt{\langle \rho^2 \rangle(0)} \equiv \frac{\rho \rho_0}{\lambda} \frac{1}{2n + |\ell| + 1},}$$

For the ground mode, n= ell=0, this is the van Cittert–Zernike theorem!

D.K., New J. Phys. **23** (2021) 033048

Magnetized stripping foil technique for ions

Examples:

1. A 100 keV proton with $n = \ell = 0$ spreads from $\rho(0) \sim 1$ Angstrom to $1 - 100$ μm:

   the needed distance is $\langle z \rangle \sim 7$ mm $-$ 70 cm, respectively.

2. For higher energies of $\varepsilon \sim 1$ MeV, the distance to spread from 1 nm to ~ 100 μm

   is $1 - 10$ meters.

Good news: $|\ell| \sim 10^2 - 10^4$

But can we really neglect scattering in the foil?
(for beams of many ions - yes)

Magnetized stripping foil technique for ions

If the final ion is an LG:

$$p_\perp \rho = 2n + |\ell| + 1,$$

$$\rho \equiv \sqrt{\langle \rho^2 \rangle}$$

$$p_\perp \equiv \sqrt{\langle p_\perp^2 \rangle}$$

Decreases as the LG packet spreads

From the Busch theorem

Assuming n << ell we get $p_\perp \approx \frac{|\ell|}{\rho} = \frac{|Z_{\rm in} - Z_{\rm out}|}{2\rho} \frac{\rho^2}{\lambda_c^2} \frac{H}{H_c},$

We require that the opening angle of the momentum cone

$$\tan \theta_0 = \tan \frac{p_\perp}{p_z} \approx \frac{p_\perp}{p_z} \ll 1,$$

be larger than the scattering angle in the foil

Magnetized stripping foil technique for ions

$\rho \sim 1 - 10\,\mu\text{m}$

$H \sim 0.5 - 1$ T,

$|Z_{\text{in}} - Z_{\text{out}}| \sim 1,$

We take light ions or protons with the energy of a few 100 keV with and get:

$$p_{\perp} \sim 0.1 - 1\,\text{keV} \qquad \underline{\theta_0 \sim 1 - 100\,\mu\text{rad}}$$

Whereas the typical scattering angles are

(https://web-docs.gsi.de/~weick/atima/atima14.html)

~ 1-100 mrad!

It this that pessimistic as it seems?

Magnetized stripping foil technique for ions

- An ion interacts with the solenoid magnetic field and a nucleus of the foil
- The scattered ions are projected on the plane waves - what defines their azimuthal angle for a thin target (carbon)?
- If the ion packet is very wide, there is no preferential angle, and the ion evolved state may not necessarily be the plane wave
- This can no longer be a pure state but a mixed one, “averaged” over impact-parameters

So, there is no solid reason to think
that the ion evolved state is a plane wave

Magnetized stripping foil technique for ions

If the final ion is an LG (pure or mixed):

$$p_\perp \rho = 2n + |\ell| + 1,$$

$$\rho \equiv \sqrt{\langle \rho^2 \rangle}$$

$$p_\perp \equiv \sqrt{\langle p_\perp^2 \rangle}$$

Defined by the scattering

From the Busch theorem

Large scattering angles imply large transverse momenta, so

1. Either it is not an LG that is generated – it can well be!
2. Or it still is an LG but with n >> ell – it is also possible!

Acceleration of charged particles with vortices and photon emission

The fields may be inhomogeneous for a beam,
but still homogeneous for an ion/proton/electron packet!

The real **in**homogeneous fields can be approximated as:

$$H_z(\rho, z) = H_z(0, z) - \frac{\rho^2}{4} H_z''(0, z) + \mathcal{O}(\rho^4),$$

$$H_\rho(\rho, z) = -\frac{\rho}{2} H'(z) + \mathcal{O}(\rho^3),$$

$$\boldsymbol{E} = E_\rho(\rho)\, \boldsymbol{e}_\rho + E_z\, \boldsymbol{e}_z,$$

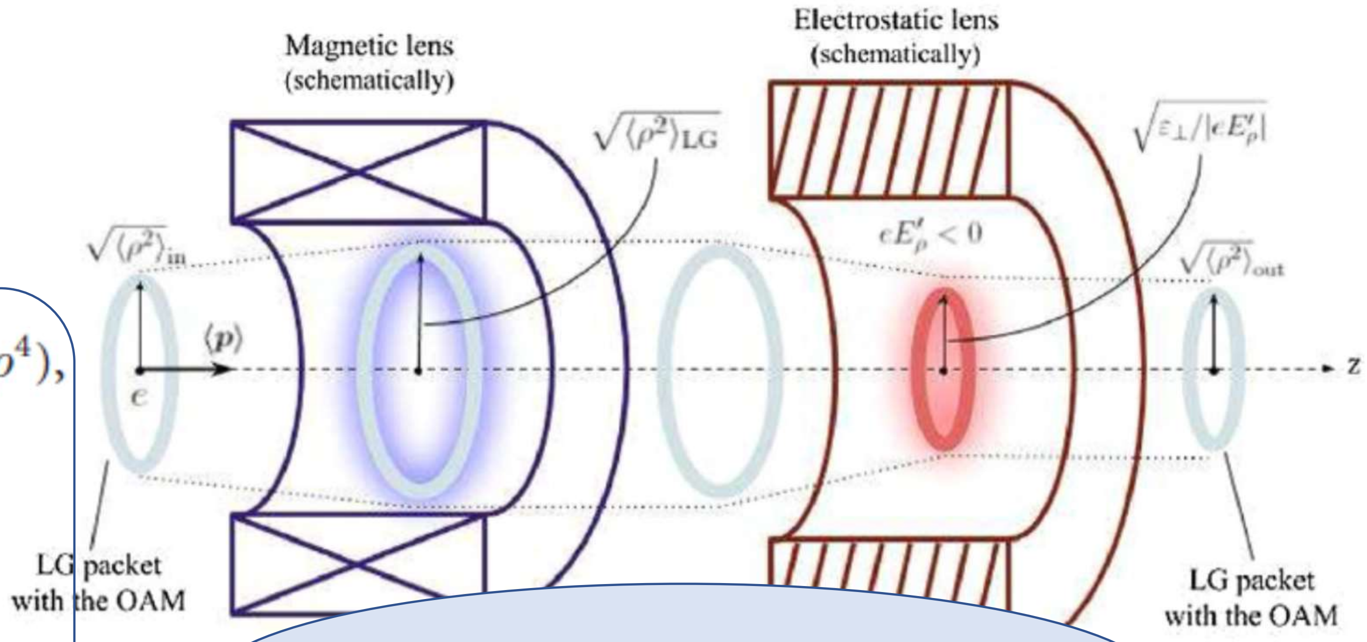

In linear fields, the OAM, the beam quality, and the emittance are conserved!

Inside a magnetic lens, the vortex electron is in the Landau state

Relativistic Landau states

$$\boldsymbol{H} = \{0, 0, H\}$$

$$H_c = 4.4 \times 10^9 \text{ T}$$

$$\Psi_i(x) = N_i^{\uparrow} \begin{pmatrix} (m+\varepsilon)\Phi_{s,\ell-1/2}(\rho)e^{-i\varphi/2} \\ 0 \\ p_z\Phi_{s,\ell-1/2}(\rho)e^{-i\varphi/2} \\ -ieH\Phi_{s,\ell+1/2}(\rho)e^{i\varphi/2} \end{pmatrix} e^{-it\varepsilon+i\ell\varphi+ip_z z}$$

The evolved photon state:

$$|\gamma\rangle_{ev} = \sum_{\lambda=\pm1}\int \frac{d^3k}{(2\pi)^3}|\boldsymbol{k},\lambda\rangle S_{fi}^{(1)} = (\varepsilon-\varepsilon')\sum_{\lambda=\pm1}\mathcal{F}\int_0^{2\pi} d\varphi_k|\boldsymbol{k},\lambda\rangle e^{i(\ell-\ell')\varphi_k}.$$

DK, Di Piazza, PRD 108, 063007 (2023); Pavlov, DK, PRD 109, 036017 (2024)

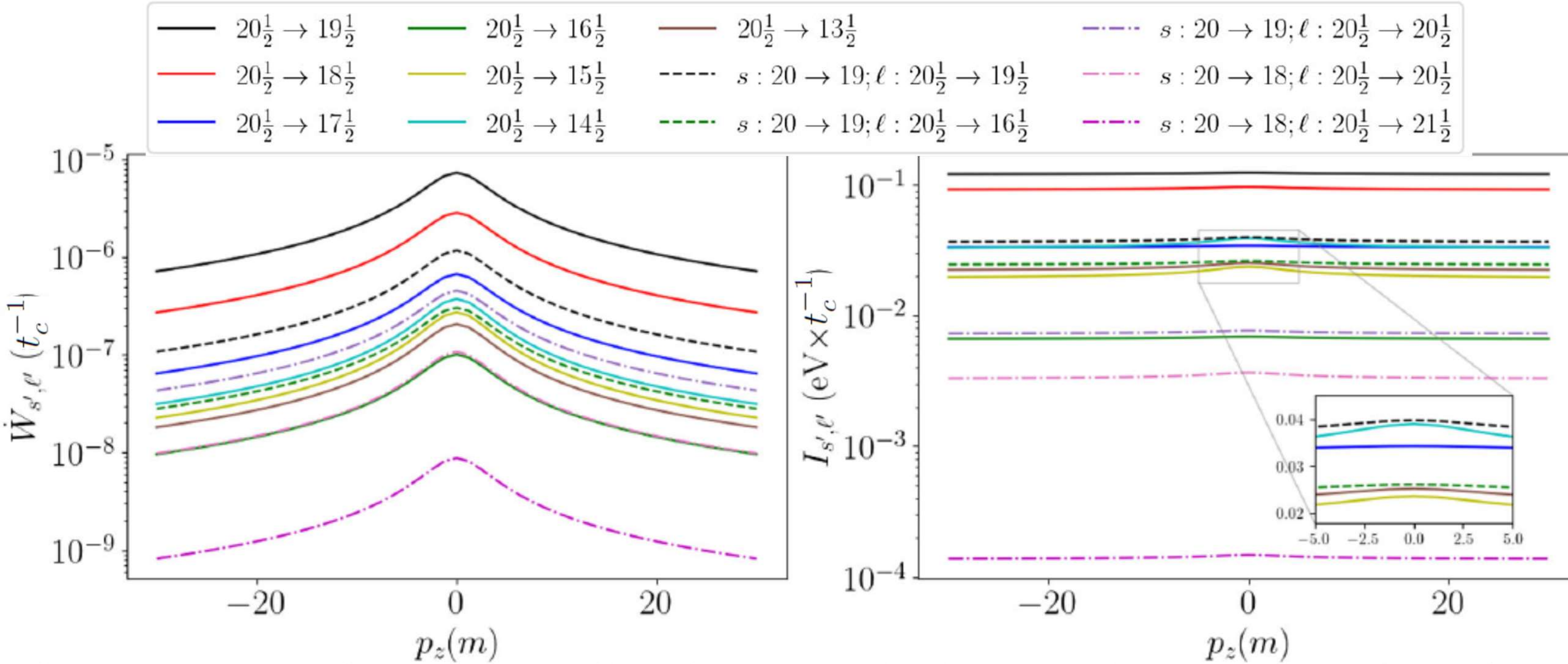

FIG. 5. The dependence of the emission probability (left) and the intensity (right) on the electron momentum p_z for $H = 0.1 H_c$, $s = s' = 20$. The transition $20\frac{1}{2} \to 19\frac{1}{2}$ means $\ell = 20\frac{1}{2}$, $\ell' = 19\frac{1}{2}$, $s = s' = 20$; those with $\ell: 20\frac{1}{2} \to 20\frac{1}{2}$ correspond to the untwisted photons with $j_z = 0$. The green line overlaps with the pink dashed one on the left; the cyan line on the left overlaps with the blue one on the right. The magenta dash-dotted line corresponds to an increase of the electron OAM during the emission (so that the photon TAM is $\ell - \ell' = -1$).

DK, Di Piazza, PRD 108, 063007 (2023); Pavlov, DK, PRD 109, 036017 (2024)

An effective time period of loosing the vorticity: s=3, p_z << m

He2

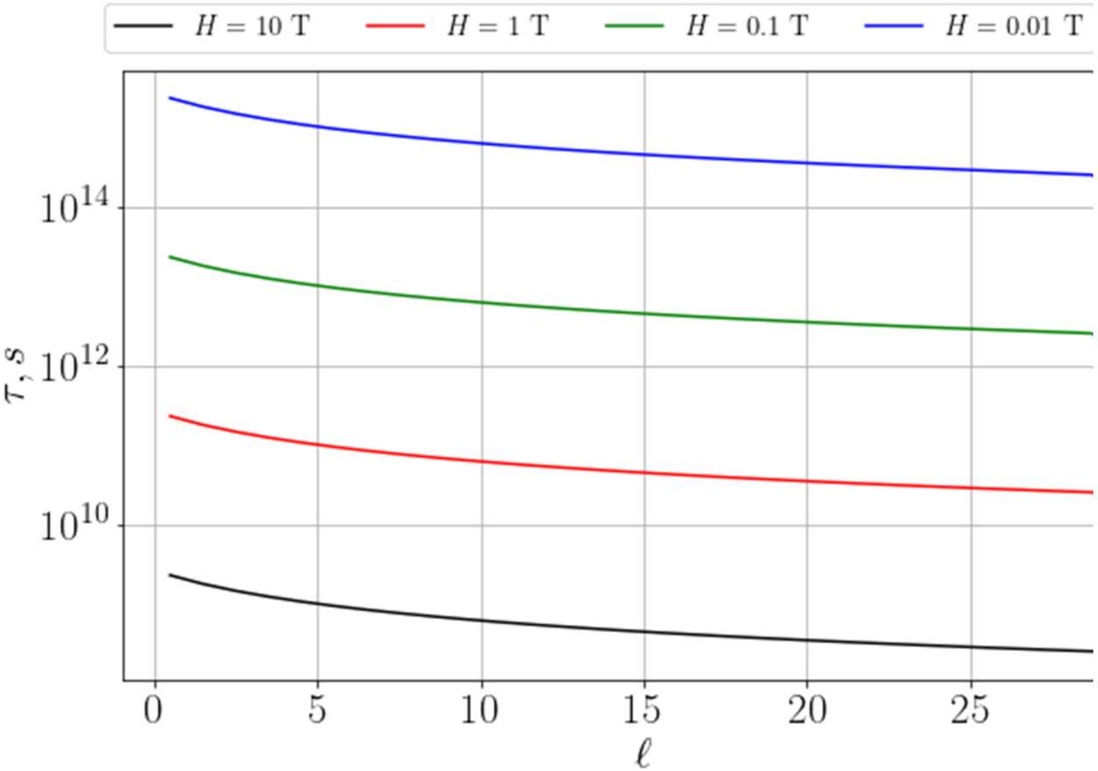

Li+

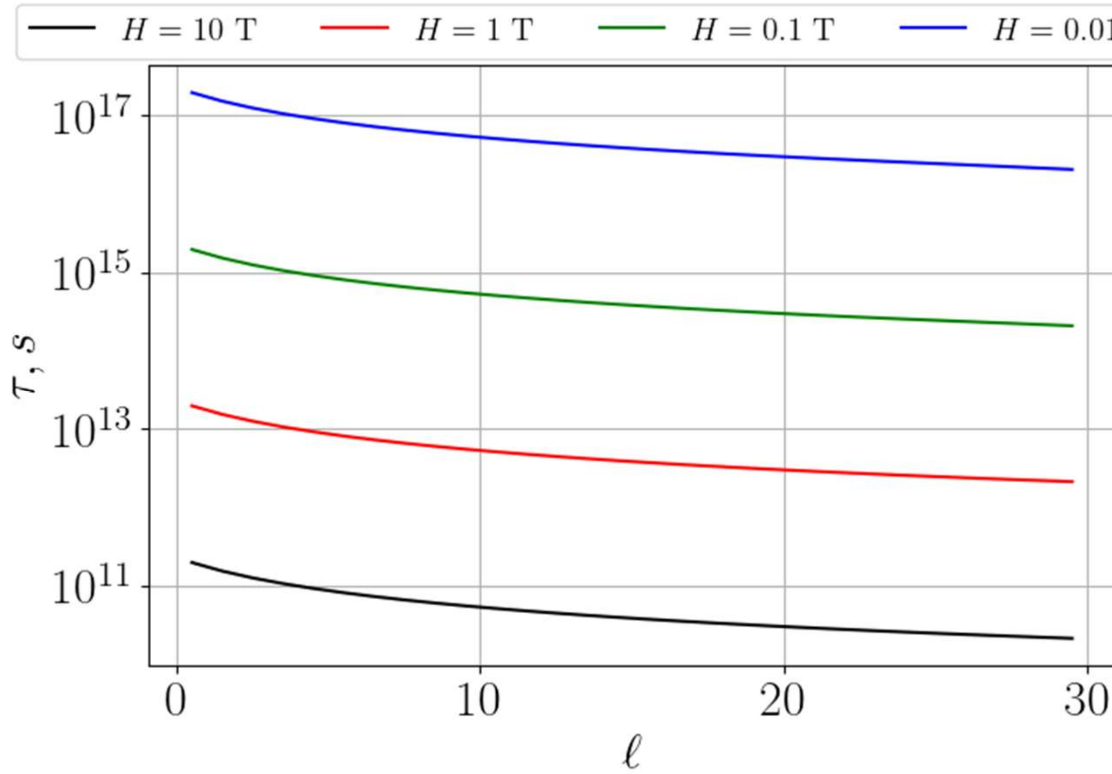

An effective time period of loosing the vorticity: s=3, p_z << m

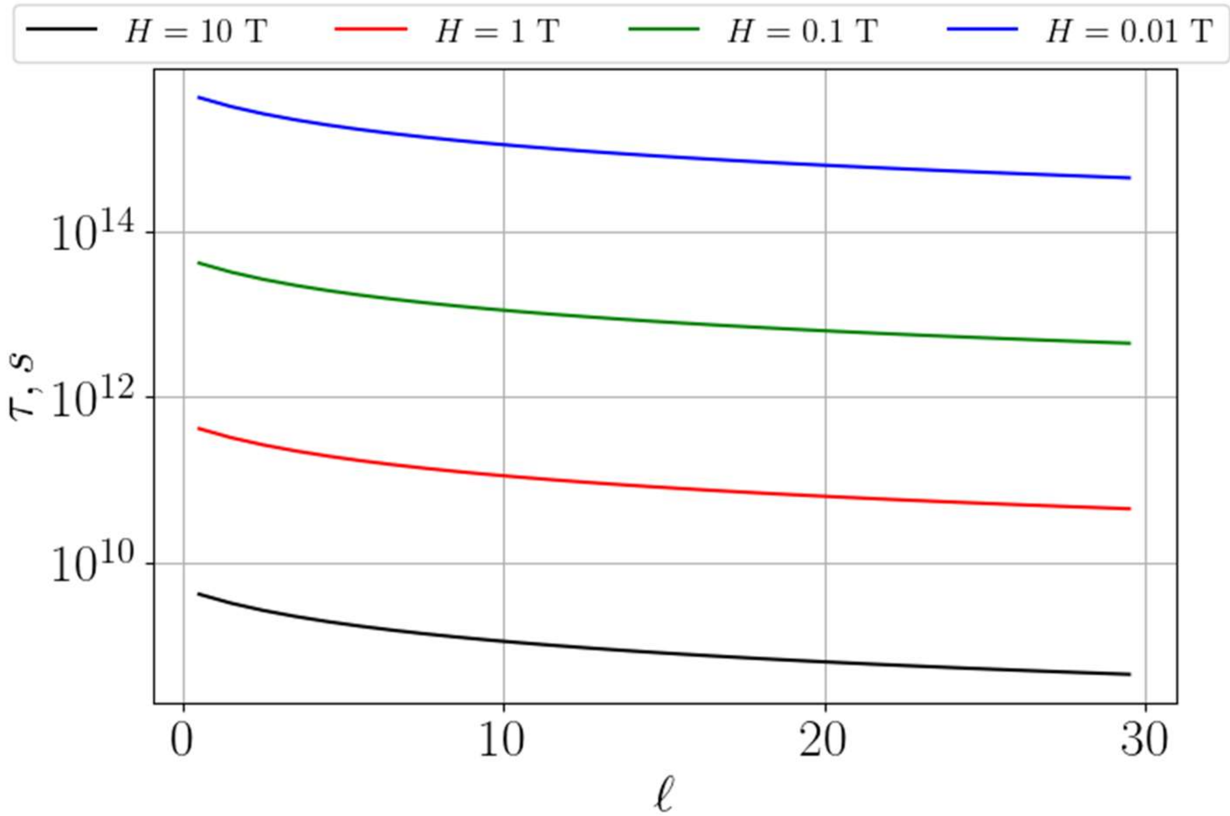

U238_37+

Listen to the talk by George Sizykh on Saturday!

On the way to experiments at accelerators….

The project of the relativistic vortex electron source

at Joint Institute for Nuclear research (Dubna):

- First at a 6-MeV electron photo-gun,
- Then at the 200-MeV linac

https://rscf.ru/en/project/23-62-10026/

Summary

1. The evolved-state formalism says if the twisted states are really generated
2. With two final particles, one can make one of them twisted by projecting the other one onto the vortex – pure or mixed – state with the OAM =0
3. This generalized-measurement technique can be used to generate vortex states of highly energetic protons, nuclei, ions, atoms, and so forth
4. Even when projecting the electron to the plane-wave, the photon state depends on a phase and on a transverse coherence of the incoming electron (quantum tomography)
5. The magnetized cathode & stripping foil techniques for electrons and ions can be tested together with more conventional methods
6. Once twisted, charged particles can be accelerated in a linac without loss of the OAM

department of PHYSICS

Thank you!

Special thanks to Andrei Surzhykov, Dima Glazov, Andrei Volotka, Valery Serbo, Igor Ivanov, Antonino Di Piazza as well to my group: George Sizykh, Alisa Chaikovskaia, Dima Grosman, Ilia Pavlov, and many others

d.karlovets@gmail.com
https://physics.itmo.ru/ru/research-group/5430